

## THE SPECTROSCOPIC ORBIT OF POLARIS, AND ITS PULSATION PROPERTIES

GUILLERMO TORRES

Center for Astrophysics | Harvard & Smithsonian, 60 Garden St., Cambridge, MA 02138, USA; gtorres@cfa.harvard.edu  
*Accepted for publication in Monthly Notices of the Royal Astronomical Society*

### ABSTRACT

Polaris is the nearest and brightest classical Cepheid, and pulsates with a period of about 4 days. It has long been known as a single-lined spectroscopic binary with an orbital period of 30 yr. Historical photometric and spectroscopic records indicate that, until recently, the pulsation period has been increasing at a rate of about  $4.5 \text{ s yr}^{-1}$ , and that the amplitude of the pulsation declined for most of the 20th century, but more recently halted its decline and began to increase. Here we report an analysis of the more than 3600 individual radial velocity measurements of Polaris available from the literature over the past 126 yr. We find that the pulsation period is now becoming shorter, and that the amplitude of the velocity variations has stopped increasing, and may be getting smaller again. We also find tantalising evidence that these changes in pulsation behaviour over the last century may be related to the binary nature of the system, as they seem to occur near each periastron passage, when the secondary comes within 29 stellar radii of the Cepheid in its eccentric orbit. This suggests the companion may be perturbing the atmosphere of the Cepheid and altering its pulsation properties at each encounter. After removal of the pulsation component of the velocities, we derive a much improved spectroscopic orbit for the binary that should serve as the basis for a more accurate determination of the dynamical masses, which are still rather uncertain.

*Keywords:* binaries: general – binaries: spectroscopic – stars: individual: Polaris – stars: oscillations – stars: variables: Cepheids – techniques: radial velocities.

### 1. INTRODUCTION

Polaris ( $\alpha$  UMi), the North Star, needs little introduction. Because of its brightness and location only  $45'$  from the north celestial pole, it has been an invaluable navigation beacon for centuries. It has also been the subject of numerous scientific investigations since the mid 1850's, when it's brightness was discovered to vary in a periodic fashion. Polaris is a yellow supergiant (F7 Ib) and a classical Cepheid, albeit a somewhat unusual one for its short period (very close to 4 days), low amplitude (currently about 0.07 mag in  $V$ ), and other characteristics of its variability. It is considered to be a first overtone pulsator (see, e.g., Feast & Catchpole 1997; Evans et al. 2002; Neilson et al. 2012).

Polaris is also a triple system. It is attended by an  $18''$  companion (Polaris B, F3 V) discovered in 1779 by William Herschel (Herschel & Watson 1782), and by a much closer spectroscopic companion (Polaris Ab, F6 V) found more than a century later by observers at the Lick Observatory, and first mentioned by Campbell (1899).<sup>1</sup> This latter companion, with its orbital period of about 30 yr, is one of the subjects of this paper. In the context of its multiplicity, we will refer to the Cepheid itself as Polaris Aa.

As the closest Cepheid to the Earth, as well as the

brightest ( $V = 2.00$ ), Polaris is an important laboratory for understanding the Cepheid phenomenon, and yet its most fundamental property — its mass — remains poorly known. This is all the more unfortunate given the long-standing discrepancy between masses predicted by stellar evolution models and by pulsation calculations, and the still few precise empirical mass measurements available for Cepheids (see, e.g., Bono et al. 2001; Neilson et al. 2011). The most recent dynamical mass estimate for Polaris Aa, relying on the binary nature of the object, is  $3.45 \pm 0.75 M_{\odot}$  (Evans et al. 2018). This determination was made possible by UV imaging observations with the Hubble Space Telescope (HST) that resolved the 30 yr spectroscopic companion for the first time (Evans et al. 2008, 2018), and by an improved parallax for the system from the Gaia DR2 catalogue (Gaia Collaboration et al. 2018).

While the radial velocity (RV) of Polaris has been monitored for a very long time, the derivation of the spectroscopic orbit has always been complicated by the fact that changes in the velocity due to the pulsation are superimposed on the long-period orbital motion, and are of comparable magnitude. It would be a relatively simple matter to account for this if the oscillations were regular, but in Polaris they are not. Both the amplitude and the period of the pulsation are changing, slowly but in an irregular and unpredictable manner over timescales of decades, or perhaps shorter. As of the most recent study from about a decade ago (Neilson et al. 2012), the pulsation period had been increasing monotonically for more

<sup>1</sup> At the time of Campbell's report, the more obvious 4-day radial velocity variability seen by the Lick astronomers, and others, was thought to be caused by an additional spectroscopic companion. The true pulsation nature of that 4-day oscillation was realised some years later.

than a century and a half at a rapid rate of about 4 or 5 seconds per year, though with an apparent “glitch” in the mid 1960s (Turner et al. 2005). More dramatic changes have been seen in the amplitude of the pulsation. Photometric and radial velocity measurements showed little or no change in the amplitude for most of the 20th century, but then a sharp decline was observed after about 1980 (Arellano Ferro 1983a; Kamper et al. 1984; Dinshaw et al. 1989; Brown & Bochonko 1994). Combined with the lengthening of the period, this drop in the amplitude fuelled speculation in the early 1990s that it might presage the complete cessation of the pulsations by 1994 or 1995 (Dinshaw et al. 1989; Fernie et al. 1993), signaling the evolution of the star out of the instability strip. This did not come to pass, however, as the pulsation amplitude first held steady at a low level in the 1990s (Kamper & Fernie 1998; Hatzes & Cochran 2000), and then began to increase again after the year 2000 (Bruntt et al. 2008; Spreckley & Stevens 2008; Lee et al. 2008). This unusual behaviour has attracted much attention over the last decade or so, and prompted detailed attempts to model the evolution of the Cepheid, but remains largely unexplained. The classical Cepheid HDE 344787, considered by some to be an analog of Polaris (Turner et al. 2010; Ripepi et al. 2021), shares many of its pulsation properties including a decreasing amplitude—now barely discernible except from space—and a rapidly increasing period. The rate of period change, however, is nearly 3 times faster than Polaris. It has also been predicted to stop pulsating in the not too distant future.

In one of the more influential spectroscopic studies of Polaris, Kamper (1996) combined an extensive series of RV measurements from the David Dunlap Observatory (1980–1995) with earlier ones from the Lick Observatory (1896–1958; Roemer 1965), and derived elements for the 30 yr single-lined spectroscopic orbit that have been widely used by many researchers since. The pulsation component of the velocities was removed from the original observations by subtracting sine curve fits from suitably grouped subsets of data. Subsequent studies by others have applied similar techniques, but have only made use of some of the available data sources to derive revised spectroscopic elements.

An exhaustive search of the literature since Kamper’s 1996 paper, and also prior to that time, has identified several new RV samples, both published and unpublished, which have not been used for the purpose of orbit determination, or to reexamine the pulsation properties. They extend the baseline up to the present, more than doubling the number of individual measurements. This new information makes it timely to return to Polaris to investigate its present status.

The structure of the paper is as follows. In Section 2 we briefly discuss the available sources of RVs for Polaris. Details of the various datasets are collected in the Appendix. Section 3 gives a description of the treatment of the velocities, and how we disentangled the pulsations from the orbital motion. The results of our analysis are reported in Section 4, beginning with the derivation of much improved elements of the spectroscopic orbit (subsection 4.1). Next we present our study of the  $O-C$  diagram, based on the RV measurements as well as on existing and new times of maximum light, revealing how the pulsation period has changed over the last 175 yr

(subsection 4.2). This is followed in Section 4.3 with our results on the changes that have occurred in the pulsation amplitude. Section 5 discusses the above results in the context of the binarity of Polaris. We conclude with final thoughts in Section 6.

## 2. RADIAL VELOCITY MATERIAL

The earliest RV measurements of Polaris of which we are aware date back to 1888 (Vogel 1895). Since then, more than two dozen publications have reported spectroscopic observations, the most extensive of which is the study by Roemer (1965), featuring nearly 1200 measurements made at the Lick Observatory over more than 60 yr. Some of the other datasets are too scattered or too poor in quality to be useful. Others have been superseded, partially or entirely, by subsequent publications in which the observations were re-reduced or their uncertainties or zeropoints changed. Table 1 lists all of the RV sources we have identified, with their Julian date range, number of original measurements, and the wavelength range of the observations, when available. They are sorted by the date of the first observation. In two cases the original measurements are unpublished, and we have obtained them from the authors. In three others, they are unavailable.

Several of the sources in Table 1 contain only relative velocities. These can still be useful for constraining the spectroscopic orbit of Polaris, provided they span a phase interval during which the orbital velocity changed significantly relative to the precision of the observations. A few of the datasets do not meet this requirement, as discussed later, and have not been considered for our analysis. The velocities reported by Dinshaw et al. (1989) are not only measured relative to the first observation, but they additionally have a quadratic approximation to the orbital motion removed. This change can be easily undone, as we describe in the Appendix, where further details of this and all other datasets are discussed. The same holds for the velocities of Kamper & Fernie (1998), which are relative and have the orbital motion subtracted. In addition to the dominant 4 d pulsation signal, a few of the studies have reported secondary periodicities in the velocities (Dinshaw et al. 1989; Hatzes & Cochran 2000; Lee et al. 2008) or are affected by seasonal variations of instrumental nature that need to be corrected (Eaton 2020; Bücke 2021). This will be described in the next section.

Figure 1 presents a visual summary of all of the observational material, which now covers more than 4 orbital cycles and contains 3727 individual RV measurements. The large scatter is caused mostly by the pulsations. As seen in the plot, there is a complete lack of useful RV measurements for two full decades, from 1960 to 1980.<sup>2</sup> This is rather unfortunate, because it is precisely during this time when there were significant changes in the characteristics of the pulsation, as we will see later.

## 3. RADIAL VELOCITY ANALYSIS

Because the velocity amplitude and period of the pulsation are not regular, removal of the 4 d oscillations from

<sup>2</sup> We have located only a handful of scattered RV measurements for Polaris from 1971 (Schmidt 1974) and 1977 (Wilson et al. 1989), but they are too few to be of use here (see the Appendix, and Table 1).

**Table 1**  
Sources of Radial Velocities for Polaris

Source	Date Range (JD−2,400,000)	Time Span (days)	$N_{\text{obs}}$	Wavelength Range
Vogel (1895)	10956–10978	22	2	Photographic, H $\gamma$ region
Roemer (1965)	13811–36505	22694	1180	Photographic, H $\gamma$ region before 1903, 4500 Å afterwards
Frost (1899)	14876–14924	48	3	Photographic
Bélopolsky (1900)	14982–15109	127	17	Photographic, H $\gamma$ region
Hartmann (1901)	15086–15403	317	35	Photographic
Küstner (1908)	16298–17016	718	7	Photographic, 4150–4500 Å
Abt (1970)	20997–27024	6027	3	Photographic, H $\gamma$ region
Henroteau (1924)	23539–23676	137	58	Photographic, 4000–4600 Å
Schmidt (1974)	40971	0	1	Photographic (Kodak 098-02), H $\alpha$ region
Wilson et al. (1989)	43297–43300	3	3	3850–4250 Å
Arellano Ferro (1983a) <sup>a</sup>	44432–44988	556	35	Photographic, mostly 4000–5000 Å, some 5300–6700 Å
Beavers & Eitter (1986)	44449	0	1	650 Å region centred at 4600 Å
Kamper et al. (1984) <sup>b</sup>	45414–45592	178	33	Photographic (IIaO, IIIaJ)
Kamper (1996) <sup>c</sup>	45414–49600	4186	307	Photographic (IIaO, IIIaJ), Reticon/CCD
Dinshaw et al. (1989)	46922–47163	241	175	4220–4700 Å
Sasselov & Lester (1990)	47432–47436	4	2	350 Å region centred at 1.1 $\mu\text{m}$
Gorynya et al. (1992)	47962–48415	453	32	4000–6000 Å
Garnavich et al. (1993) <sup>d</sup>	1992–	...	...	Hydrogen fluoride cell, 8600 Å
Hatzes & Cochran (2000)	48581–49201	620	42	23.6 Å region centred at 5520 Å
Gorynya et al. (1998)	49446–49569	123	40	4000–6000 Å
Usenko et al. (2015)	49512–54934	5422	56	5800–6800 Å, 5500–7000 Å, 4470–7100 Å
Kamper & Fernie (1998)	49950–50568	618	212	6290 Å after early 1994
Eaton (2020)	52998–55138	2140	679	5000–7100 Å
Lee et al. (2008) <sup>e</sup>	53332–54269	937	265	$I_2$ cell, $\sim$ 5000–6000 Å
Bücke (2021) <sup>e</sup>	53482–60005	6523	296	6050–6700 Å
Fagas et al. (2009) <sup>f</sup>	Dec2007–Jul2008	...	330	...
De Medeiros et al. (2014) <sup>f</sup>	...	6098	13	3600–5200 Å
Anderson (2019)	55816–58443	2627	161	4813–6476 Å
Usenko et al. (2016)	57283–57376	93	21	4900–6800 Å
Usenko et al. (2017)	57623–57816	193	49	4900–6800 Å
Usenko et al. (2018)	57971–58248	277	63	4900–6800 Å
Usenko et al. (2020)	58368–58955	587	53	4900–6800 Å

**Note.** — Measurements by Vogel (1895), Frost (1899), Abt (1970), Schmidt (1974), Wilson et al. (1989), Beavers & Eitter (1986), and Sasselov & Lester (1990) are either poor, too few, or too scattered to be useful.

<sup>a</sup> Most of these measurements were superseded by the publication of Kamper (1996), in which a  $+0.5 \text{ km s}^{-1}$  offset was applied.

<sup>b</sup> All of these measurements were superseded by the publication of Kamper (1996).

<sup>c</sup> Some of these measurements were superseded by the publication of Kamper & Fernie (1998).

<sup>d</sup> No other details or individual RVs were published.

<sup>e</sup> Unpublished measurements kindly provided by the author.

<sup>f</sup> Unpublished. Only the time interval or time span was reported.

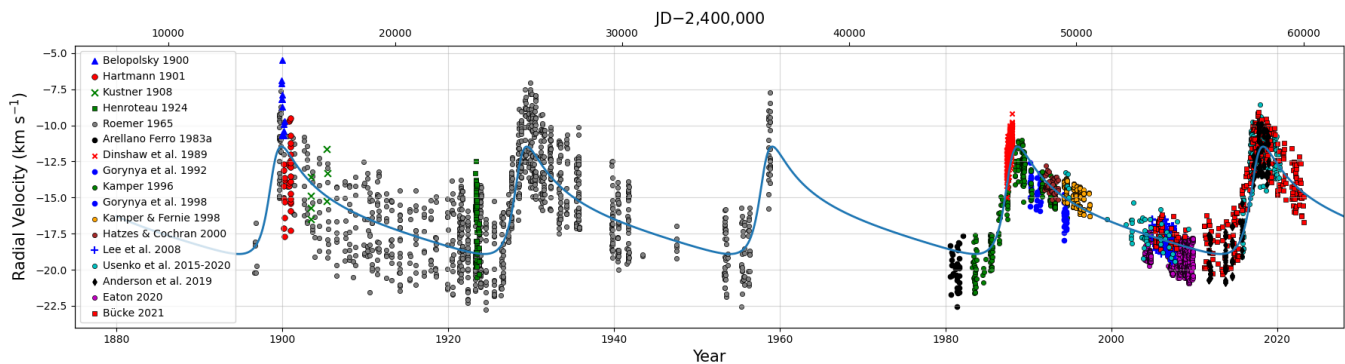


**Figure 1.** Historical radial velocities of Polaris, shown with the orbital model by Kamper (1996) for reference. The large scatter is caused by the pulsation motion, which is superimposed on the orbital motion. Datasets reporting relative velocities have been shifted by eye to bring them in line with the others.

the original RV data in order to study the orbital motion requires us to determine the properties of the pulsation as part of the process. The procedure we followed is iterative, alternating between refining the pulsation properties and improving the orbital solution. As is customary in the study of variable stars, we relied on the  $O-C$  diagram to investigate changes in the pulsation period. This diagram typically shows the difference between observed times of maximum light and calculated times based on a fixed linear ephemeris. In this case, we are dealing with radial velocities rather than brightness measurements, but it has been found that the velocity minima for small-amplitude pulsating yellow supergiants such as Polaris correspond quite closely to light maxima, with only a modest time shift (Arellano Ferro 1983b). The study of Turner et al. (2005) established the offset to be  $-0.383$  d, which they added to their measured times of minimum RV in order to align them with the times of maximum light. A smaller adjustment of  $-0.21$  d was advocated by Arellano Ferro (1983a), and Kamper & Fernie (1998) adopted an intermediate value of  $-0.333$  d. As we show later in Section 4.2, the value of  $-0.21$  d seems more consistent with our measurements, and is adopted for this paper.

For the present analysis we followed Turner et al. (2005), and others, in adopting the ephemeris of Berdnikov & Pastukhova (1995) for the times of maximum light:

$$\text{HJD}_{\text{max}} = 2,428,260.727 + 3.969251E, \quad (1)$$

where  $E$  represents the number of cycles elapsed since the reference epoch.

We began by subtracting from the original velocities the orbital motion predicted from the elements reported by Kamper (1996). Datasets with relative velocities were offset by eye so as come close to others near in time. All dates of observation were corrected for light travel time in the 30 yr orbit to refer them to the barycentre of the binary, based on the same set of orbital elements. In this case those corrections are small, and range from  $-0.025$  d to  $+0.007$  d throughout the orbit. As in most Cepheids of low amplitude, the brightness and velocity variations in Polaris are very nearly sinusoidal (see, e.g., Efremov 1975), which makes the process of subtracting out the pulsation simpler. However, prior to that step, we removed additional periodicities or other spurious variations in some of the datasets so as to avoid extra scatter. For example, Dinshaw et al. (1989) reported a secondary period of about 45 d in their data. In this case we chose to fit the sum of two sinusoids (for the 4 d pulsation component, and the 45 d component), allowing the periods and amplitudes to vary, and then subtracted only the 45 d component from the orbit-corrected velocities, leaving just the pulsations. We proceeded similarly with a 40 d signal found by Hatzes & Cochran (2000), and a 119 d signal reported by Lee et al. (2008). The Eaton (2020) RVs showed a fairly obvious annual pattern in the residuals of unknown origin. We removed it in the same way.<sup>3</sup> The velocities of Bücke (2021) are affected by seasonal variations related to thermal effects in their

<sup>3</sup> Anderson (2019) carried out a search for additional periodicities in their spectroscopic observations by examining the line bisectors, rather than the velocities, because this avoids complications from the orbital motion as the bisectors should be unaffected.

instrumentation (see the Appendix). In this case, we first removed the pulsation component and then fitted the residuals with a spline function, and subtracted this spline fit from the orbit-corrected data. This left only the changes due to pulsation.

With the orbital motion removed, and any additional periodicities also removed as just described, we then divided each dataset into subsets in time, and fitted a sine curve to the RVs in each interval to model the pulsation. We solved for the amplitude of the pulsation variation ( $A_{\text{puls}}$ ), the time of velocity minimum nearest to the average date of each interval ( $T_{\text{min}}$ ), and a velocity offset. The period was initially held fixed at the value in eq.[1]. The definition of these intervals, particularly for some of the sources with sparse sampling, was a compromise between having enough observations to sample the pulsation cycle, and a time span short enough to not smear out real evolution in the amplitude or phasing. The median number of observations per interval is about two dozen, and the median duration is about two months, although there is a significant range in both, depending on the dataset. Because the period is changing, this step of modelling the pulsation with a sine function was repeated after the initial fit, using the resulting  $O-C$  diagram to predict a more accurate period at the mean epoch of each interval, and holding it fixed.

The next step in our analysis was to subtract these sine curve fits (and the additional periodicities mentioned earlier) from the original RV data, which left only the orbital motion plus any shifts due to differences in the velocity zeropoints of the various datasets. This was then used to solve for the spectroscopic orbital elements, the details of which we describe in the next section. The entire process in this section was repeated several times until convergence, during which a small number of RV outliers were rejected. We retained a total of 3659 measurements. As a result of this effort, we obtained improved elements for the 30 yr orbit of Polaris, as well as a set of homogeneous measurements that trace the evolution of the period and velocity amplitude of the pulsations over more than a century. The  $O-C$  and RV amplitude measurements we obtained are presented in Table 2, along with other properties of the fits, and will be discussed below.

## 4. RESULTS

### 4.1. Revised Spectroscopic Orbital Solution

The radial velocities of Polaris, modified as described above to remove all contributions except for the orbital motion, span more than 126 yr, or 4.3 orbital cycles. They are listed in Table 3, together with their formal uncertainties. The measurements of Arellano Ferro (1983a) and Kamper (1996), obtained at the same observatory, were merged and treated as a single dataset for our analysis, after applying an offset of  $+0.5 \text{ km s}^{-1}$  to the former velocities to place them on the same reference frame as the latter (see the Appendix). We also grouped to-

Aside from the pulsations, they found evidence for a 40 d variation (the same as in Hatzes & Cochran 2000) and a 60 d variation, although they had reservations about the latter signal. While it is not a goal of this paper to perform a detailed search for other periodicities in the published RVs, our two-component sine fit to the Anderson (2019) velocities did not reveal a signal at 40 d with an amplitude significant enough to affect our results, so for our purposes we have not considered that signal further.

**Table 2**  
Spectroscopic Amplitude and Timing Measurements for Polaris

Mean JD (HJD−2,400,000)	JD Interval (HJD−2,400,000)	$N_{\text{obs}}$	$E$	$A_{\text{puls}}$ ( $\text{km s}^{-1}$ )	$T_{\text{min}}$ (HJD−2,400,000)	$\Delta t$ (day)	$O-C$ (day)	RMS ( $\text{km s}^{-1}$ )	Source
13850.280	13812–13903	7	−3632	$2.506 \pm 0.170$	$13847.486 \pm 0.028$	+0.005	3.079	0.218	1
14895.563	14876–14911	21	−3368	$2.882 \pm 0.153$	$14895.025 \pm 0.035$	+0.002	2.736	0.496	1
14996.439	14945–15094	13	−3343	$3.283 \pm 0.228$	$14994.196 \pm 0.038$	+0.001	2.676	0.511	1
15042.930	14988–15109	13	−3331	$1.944 \pm 0.350$	$15042.205 \pm 0.126$	0.000	3.053	0.866	2
15105.995	15086–15134	12	−3315	$2.497 \pm 0.838$	$15105.270 \pm 0.176$	−0.001	2.610	1.782	3

**Note.** — Cycle numbers ( $E$ ) are based on the ephemeris in eq.[1]. Column  $A_{\text{puls}}$  gives the velocity semi-amplitude. Column  $T_{\text{min}}$  contains the measured times of RV minimum, corrected for the light travel time  $\Delta t$  in the following column, and shifted by  $-0.21$  d to line up with the times of maximum light (see the text). The  $O-C$  residuals are computed from  $T_{\text{min}}$ , the cycle number, and the ephemeris. The scatter of each sine curve fit is given in column RMS. Sources in the last column are as follows: (1) Roemer (1965); (2) B elopolsky (1900); (3) Hartmann (1901); (4) K ustner (1908); (5) Henroteau (1924); (6) Arellano Ferro (1983a); (7) Kamper (1996); (8) Dinshaw et al. (1989); (9) Gorynya et al. (1992); (10) Hatzes & Cochran (2000); (11) Gorynya et al. (1998); (12) Usenko et al. (2015, 2016, 2017, 2018, 2020); (13) Kamper & Fernie (1998); (14) Eaton (2020); (15) Lee et al. (2008); (16) B ucke (2021); (17) Anderson (2019). (This table is available in its entirety in machine-readable form)

**Table 3**  
Radial Velocities for Polaris with the Pulsation Removed

Date <sup>a</sup> (HJD)	Year	$\Delta t$ (day)	RV ( $\text{km s}^{-1}$ )	$\sigma_{\text{RV}}$ ( $\text{km s}^{-1}$ )	Source
2413811.956	1896.6926	+0.004	−17.706	0.500	1
2413818.953	1896.7117	+0.004	−17.999	0.500	1
2413826.897	1896.7335	+0.005	−17.907	0.500	1
2413838.878	1896.7663	+0.005	−17.897	0.500	1
2413875.810	1896.8674	+0.005	−18.054	0.500	1

**Note.** — The RVs in the table are listed as used in our orbital analysis. The sources, which are numbered differently than in Table 2 because some of the datasets were merged for the orbital analysis and others were omitted, are as follows: (1) Roemer (1965); (2) Hartmann (1901); (3) K ustner (1908); (4) Arellano Ferro (1983a) +  $0.5 \text{ km s}^{-1}$ , and Kamper (1996); (5) Dinshaw et al. (1989); (6) Gorynya et al. (1992, 1998); (7) Hatzes & Cochran (2000); (8) Usenko et al. (2015), Usenko et al. (2016), Usenko et al. (2017), Usenko et al. (2018), and Usenko et al. (2020); (9) Kamper & Fernie (1998); (10) Eaton (2020); (11) Lee et al. (2008); (12) B ucke (2021); (13) Anderson (2019). The formal uncertainties listed are as published, or assigned here when not published (see the Appendix). Those of Dinshaw et al. (1989) and Usenko were found to be overestimated, and have been reduced by a factor of 5 from their reported values. For the final uncertainties used in our orbital analysis, see Table 5. (This table is available in its entirety in machine-readable form)

<sup>a</sup> Dates have been corrected for light travel time to the barycentre of the Polaris Aa+Ab system, using the orbital elements in Table 4. The corrections  $\Delta t$  are listed in the third column.

gether the RVs of Gorynya et al. (1992, 1998), which were made with the same instrumentation and measuring technique. Similarly, the RVs of Usenko and collaborators, published in several batches over a period of 5 yr, were combined and considered as one group (Usenko et al. 2015, 2016, 2017, 2018, 2020). In total we used 13 separate RV datasets. The uncertainties were initially adopted as published, and in cases where errors were not reported, we assigned reasonable values. We refer the reader to the Appendix for the details of each set.

The six standard elements of a single-lined spectroscopic orbit were solved with a Markov chain Monte Carlo (MCMC) procedure, using the EMCEE<sup>4</sup> package of Foreman-Mackey et al. (2013). The eccentricity and argument of periastron were cast as  $\sqrt{e} \cos \omega$  and  $\sqrt{e} \sin \omega$ , in which  $\omega$  is the value for the primary (star Aa). Additionally, to account for differences in the velocity zero-

points of the various datasets, we included 12 free parameters representing offsets relative to the Roemer (1965) velocities, which are the most numerous and have the longest baseline. The MCMC chains had 10,000 links after burn-in, and the priors adopted for the adjustable parameters were all uniform over suitable ranges. Convergence was checked by inspecting the chains visually, and by requiring a Gelman-Rubin statistic of 1.05 or smaller (Gelman & Rubin 1992).

Initial solutions indicated many of the datasets had velocity uncertainties that are underestimated, based on their  $\chi^2$  values. In two cases (Dinshaw et al. 1989, and the Usenko velocities) they appeared to be significantly overestimated. We first scaled down the errors for those two groups arbitrarily by a factor of 5, and then allowed for an additional source of uncertainty in each of the 13 datasets by solving for separate ‘‘jitter’’ values, added quadratically to the formal uncertainties. This extra jitter may be caused in part by unstable zero-points within each dataset, by imperfect modelling and subtraction of the pulsation variation, or by other unrecognised periodicities.

The resulting orbital elements are presented in Table 4, and the velocity offsets and jitter terms are given separately in Table 5. A plot of the velocities and our model is seen in Figure 2, in which all offsets listed in Table 5 have been applied. The scale is the same as in Figure 1, and shows the reduction in the scatter after the removal of the pulsation variation. Correlations among the standard orbital elements are shown in Figure 3.

#### 4.2. Period Variations and the $O-C$ Diagram

Changes in the period of pulsation of Polaris have long been known from the work of visual observers (e.g., Stebbins 1946), and were shown clearly also in the extensive RV measurements by Roemer (1965) (see her Figure 46). Most observers have concluded that the period has been increasing at a fairly constant rate between 3 and  $5 \text{ s yr}^{-1}$ , based on a quadratic fit to the  $O-C$  diagram. Some authors have drawn attention to deviations from that shape, and have suggested 5th order or even 7th order approximations (Fernie et al. 1993; Kamper & Fernie 1998). In a comprehensive review of the existing material for Polaris, Turner et al. (2005) remeasured the timings from all available visual, photometric, and RV observations going back to 1844, and up to 2004. They

<sup>4</sup> <https://emcee.readthedocs.io/en/stable/index.html>

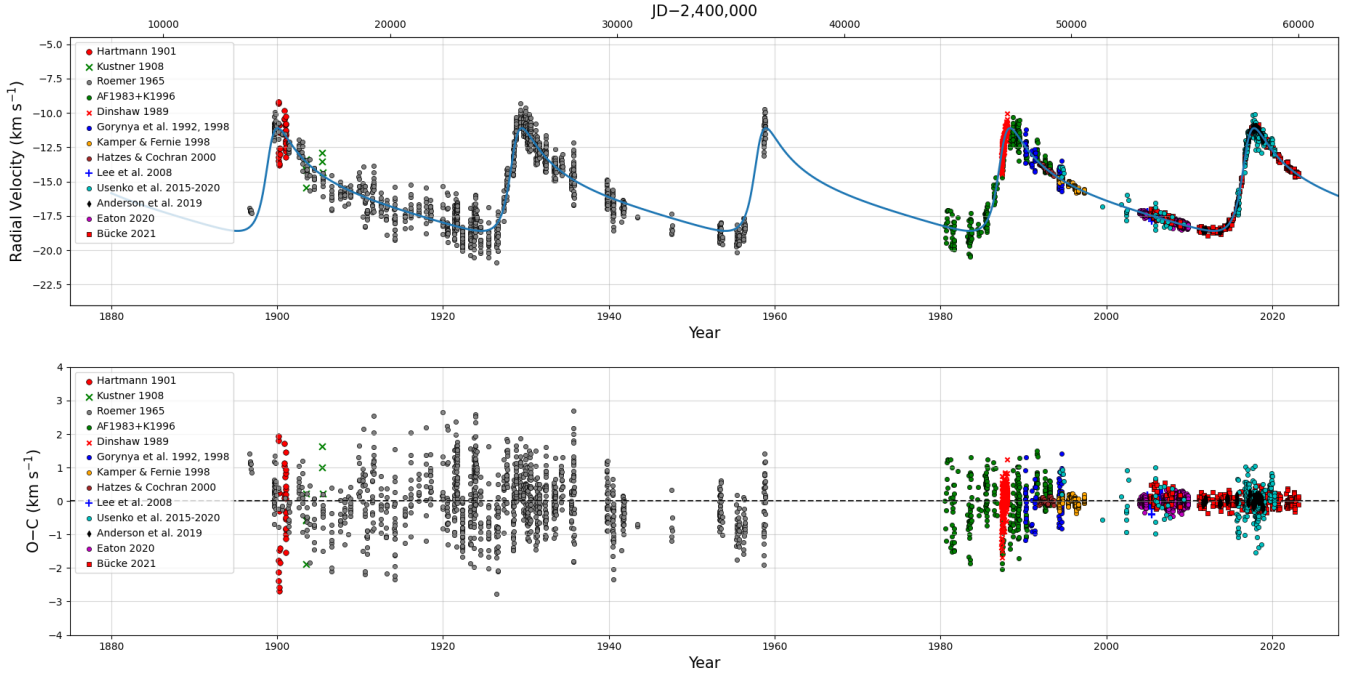


**Figure 2.** Radial velocities of Polaris disaffected from the pulsation variations, and adjusted for the offsets given in Table 5. The “AF1983+K1996” dataset combines the Arellano Ferro (1983a) velocities adjusted by  $+0.5 \text{ km s}^{-1}$ , and those of Kamper (1996). The curve is our model from Table 4. Compare with Figure 1. Velocity residuals are shown at the bottom on an expanded scale.

**Table 4**  
Updated Spectroscopic Orbital Elements for Polaris

Parameter	Value
$P$ (yr)	$29.4330 \pm 0.0079$
$\gamma$ ( $\text{km s}^{-1}$ )	$-16.084 \pm 0.025$
$K$ ( $\text{km s}^{-1}$ )	$3.7409 \pm 0.0075$
$\sqrt{e} \cos \omega$	$+0.4175 \pm 0.0040$
$\sqrt{e} \sin \omega$	$-0.6672 \pm 0.0026$
$T_{\text{peri}}$ (yr)	$2016.801 \pm 0.011$
Derived properties	
$e$	$0.6195 \pm 0.0015$
$\omega$ (degree)	$302.04 \pm 0.34$
$M_{\text{Ab}} \sin i / (M_{\text{Aa}} + M_{\text{Ab}})^{2/3} (M_{\odot})$	$0.30442 \pm 0.00075$
$a_{\text{Aa}} \sin i (10^6 \text{ km})$	$434.1 \pm 1.1$

**Note.** — The values listed correspond to the mode of the posterior distributions, with their 68.3% credible intervals, which are symmetrical in all cases. The centre-of-mass velocity  $\gamma$  uses the Roemer (1965) dataset as the reference. The last two lines give the coefficient of the minimum secondary mass, and the linear semimajor axis of the primary.

concluded that the period has been monotonically increasing at a rate of approximately  $4.5 \text{ s yr}^{-1}$ , but with a brief interruption between about 1963 and 1966, during which it appeared to have suddenly decreased. The period then resumed its increase at about the same rate as before. Other authors have followed Turner et al. (2005) in showing separate parabolic fits to the timings in the  $O-C$  diagram before and after 1965, and have reported that new measurements until 2011 still appear to fit the more recent trend fairly well (e.g., Neilson et al. 2012).

Figure 4 reproduces the photometric and spectroscopic  $O-C$  measurements from the work of Turner et al. (2005), to which we have added the subset of our own spectroscopic values from Table 2 after 2005. The curves

**Table 5**  
Radial Velocity Offsets and Jitter Values

Source	RV Offset ( $\text{km s}^{-1}$ )	RV Jitter ( $\text{km s}^{-1}$ )
(1) Roemer (1965) <sup>a</sup>	...	$0.681^{+0.022}_{-0.022}$
(2) Hartmann (1901)	$+1.39^{+0.19}_{-0.18}$	$0.51^{+0.24}_{-0.26}$
(3) Küstner (1908)	$+1.05^{+0.51}_{-0.52}$	$0.75^{+0.80}_{-0.45}$
(4) Arellano Ferro (1983a) <sup>b</sup>	$+1.027^{+0.043}_{-0.043}$	$0.524^{+0.032}_{-0.029}$
(5) Dinshaw et al. (1989)	$-11.829^{+0.050}_{-0.051}$	$0.469^{+0.031}_{-0.026}$
(6) Gorynya et al. (1992) <sup>c</sup>	$+1.488^{+0.069}_{-0.070}$	$0.500^{+0.053}_{-0.045}$
(7) Hatzes & Cochran (2000)	$-14.117^{+0.030}_{-0.030}$	$0.027^{+0.019}_{-0.016}$
(8) Usenko et al. (2015) <sup>d</sup>	$+0.068^{+0.042}_{-0.042}$	$0.387^{+0.028}_{-0.026}$
(9) Kamper & Fernie (1998)	$-0.222^{+0.028}_{-0.028}$	$0.1061^{+0.0070}_{-0.0060}$
(10) Eaton (2020)	$+1.120^{+0.027}_{-0.026}$	$0.0444^{+0.0078}_{-0.0110}$
(11) Lee et al. (2008)	$-17.794^{+0.027}_{-0.028}$	$0.1103^{+0.0054}_{-0.0046}$
(12) Bücke (2021)	$-18.387^{+0.027}_{-0.027}$	$0.0976^{+0.0110}_{-0.0094}$
(13) Anderson (2019)	$+0.551^{+0.027}_{-0.027}$	$0.0977^{+0.0064}_{-0.0054}$

**Note.** — The values listed correspond to the mode of the posterior distributions, with their 68.3% credible intervals. The offsets are to be added to each dataset to place the RVs on the frame of the Roemer (1965) velocities. The RV jitter values are added quadratically to the internal errors. Sources are numbered as in Table 3.

<sup>a</sup> Reference dataset for all RV offsets.

<sup>b</sup> This dataset includes the velocities of Kamper (1996).

<sup>c</sup> This dataset includes the velocities of Gorynya et al. (1998).

<sup>d</sup> This dataset includes the velocities of Usenko et al. (2016, 2017, 2018, 2020).

displayed are our weighted quadratic fits to the Turner et al. (2005) measurements, before and after 1965. The most recent of our data after about 2012 show a clear de-

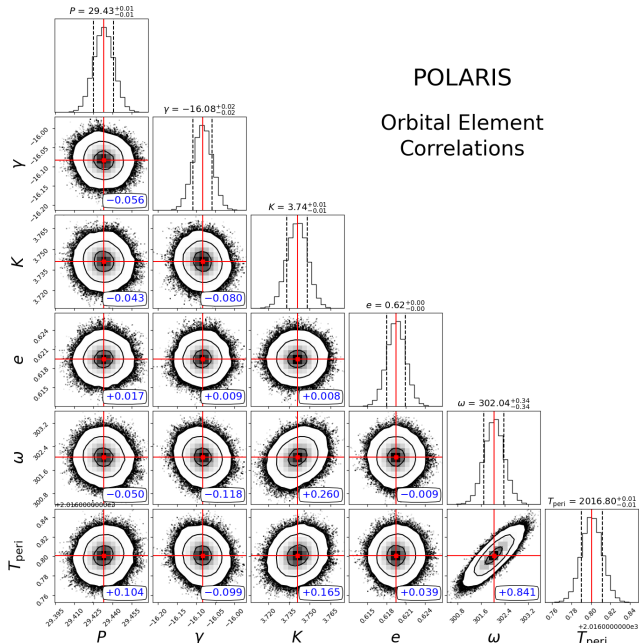


**Figure 3.** Corner plot for the standard orbital elements of Polaris, showing the correlations. The contours correspond to confidence levels of 1, 2, and  $3\sigma$ , and the values in each panel are the correlation coefficients.

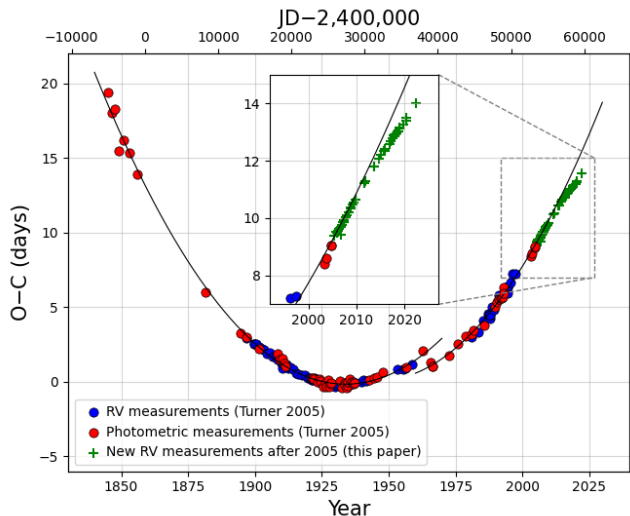


**Figure 4.**  $O-C$  diagram for Polaris based on visual, photoelectric, and spectroscopic timing measurements by Turner et al. (2005). New spectroscopic values after 2005 are added from the present work. The curves are weighted quadratic fits to the Turner et al. (2005) data before and after 1963 (excluding our own), implying fairly consistent period increases of  $dP/dt = 4.45 \pm 0.04$  and  $5.07 \pm 0.57$  s  $\text{yr}^{-1}$ , respectively. The new spectroscopic data show an obvious departure from the fit after about 2012.

parture from the quadratic fit, implying the period has stopped increasing and is now becoming shorter. Early indications of this were discussed by Spreckley & Stevens (2008), based on photometric observations collected by the Solar Mass Ejection Imager (SMEI) instrument on board the Coriolis satellite, between 2003 and 2007.

We used an updated version of the  $O-C$  diagram to infer the instantaneous values of the pulsation period as a function of time. The data for this diagram included all

**Table 6**  
New Times of Maximum Light from TESS

BJD (2,400,000+)	$\Delta t$ (day)	$E$	$O - C$ (day)
58817.473	-0.011	7695	$13.349 \pm 0.025$
58821.472	-0.011	7696	$13.378 \pm 0.025$
58825.434	-0.011	7697	$13.371 \pm 0.025$
58829.255	-0.011	7698	$13.223 \pm 0.025$
58833.365	-0.011	7699	$13.364 \pm 0.025$

**Note.** — The  $\Delta t$  values in column 2 are the additive light travel time corrections to reduce the measured times of maximum light in column 1 to the barycentre of the 30 yr binary. Cycle numbers  $E$  are counted from the reference epoch given in eq.[1]. (This table is available in its entirety in machine-readable form).

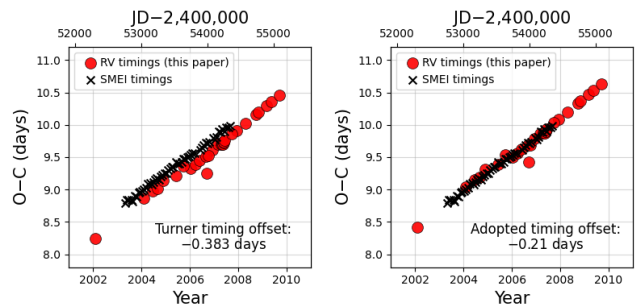


**Figure 5.** Determination of the optimal shift to be applied to our measured times of minimum RV in order to align them with the times of maximum brightness from the SMEI observations (Spreckley & Stevens 2008). The  $O-C$  diagram on the left uses the offset adopted by Turner et al. (2005) to adjust the RV timings. The one on the right uses the value of  $-0.21$  d advocated by Arellano Ferro (1983a), and clearly works best for our data.

our newly derived spectroscopic timings from Table 2, the photometric measurements of Turner et al. (2005), and the highly precise times of maximum light from the SMEI instrument by Spreckley & Stevens (2008). Those timings are contemporaneous with some of our spectroscopic determinations, and support a value for the offset between the times of velocity minima and light maxima of  $-0.21$  d (see Figure 5), as found by Arellano Ferro (1983a). We applied this value to all our spectroscopic timings to align them with the photometric values. We have also added 3 photometric timings by Bruntt et al. (2008) from the WIRE satellite, and 5 photometric timings by Neilson et al. (2012), extracted by digitising their Figure 1. In addition, Polaris has been observed by the Transiting Exoplanet Survey Satellite (TESS; Ricker et al. 2015) in several sectors (#19, 20, 25, 26, 40, 47, 52, 53, and 60, as of this writing). We downloaded the photometry from the Mikulski Archive for Space Telescopes (MAST)<sup>5</sup>, and measured the times of maximum light by fitting a sine function to the top half of each cycle.<sup>6</sup>

<sup>5</sup> <https://archive.stsci.edu/>

<sup>6</sup> Because Polaris is such a bright star, it saturates the TESS detectors and causes “bleed trails” extending many CCD rows above and below the saturated pixels. This requires very large photometric apertures in order to capture all the flux (see <https://heasarc.gsfc.nasa.gov/docs/tess/observing-technical.html>), and makes it difficult to extract precise photometry from these observations, particularly as the extent of the bleed trails may vary along the pulsation cycle. While we do not expect this to bias our determination of the times of maximum

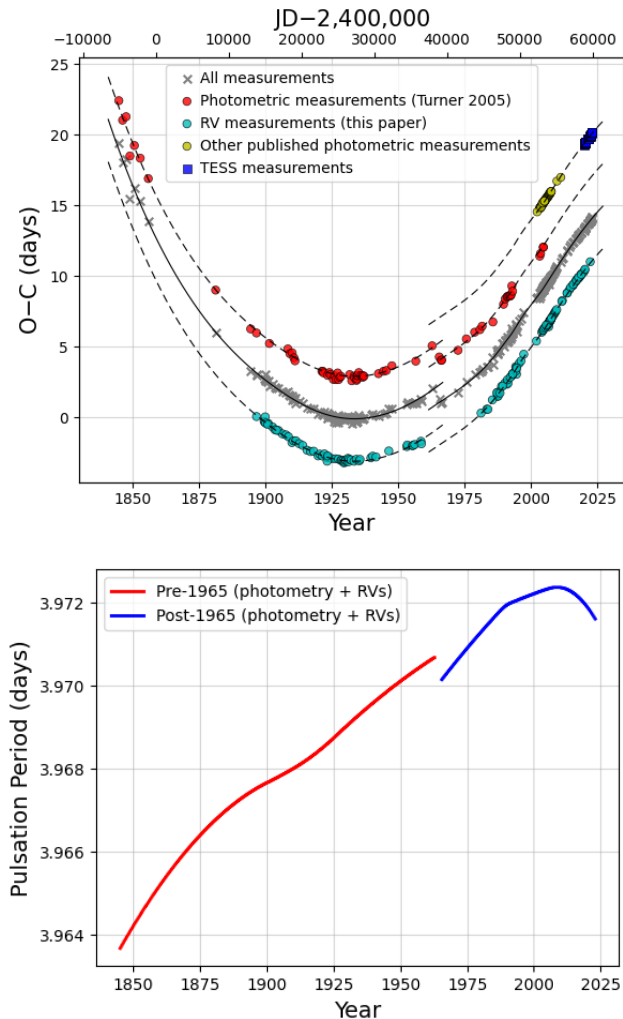


**Figure 6.** Top: Updated  $O-C$  diagram for Polaris (grey crosses) that includes the visual and photoelectric timing measurements by Turner et al. (2005), our own spectroscopically determined timings from Table 2, the SMEI timings from Spreckley & Stevens (2008), 3 additional measurements by Bruntt et al. (2008) from the WIRE satellite, and 5 others by Neilson et al. (2012). The solid curves pre- and post-1965 are spline fits to the data. The photometric and spectroscopic timings are also shown separately to illustrate their time coverage, by plotting them in parallel sequences (dashed lines) offset vertically from the central sequence (crosses) for clarity. Bottom: The time-dependent instantaneous pulsation period derived from the  $O-C$  diagram, before and after the interruption in 1965.

These 52 new measurements are listed in Table 6.

All of the additional times of maximum light mentioned above were corrected for light travel time, for consistency. The updated  $O-C$  diagram is shown in the top panel of Figure 6, along with spline fits to the data before and after the 1965 break. Using these spline fits, we derived a smooth representation of the evolution of the instantaneous pulsation period over the last 175 yr, which is shown in the lower panel. A turnover is seen to have occurred around 2010, and the period is now becoming shorter. The sudden drop in 1965 is close to a minute, and the total change between 1845 and the max-

brightness, it may compromise the determination of light amplitudes, and for this reason we do not use the TESS photometry in the next section for that purpose.

imum around 2010 is about 12 minutes, corresponding to an average of  $\sim 4.5 \text{ s yr}^{-1}$ , as found previously.

The sharpness and amplitude of the decline in the mid 1960s reported by Turner et al. (2005) rely strongly on a single measurement of a time of maximum brightness from late 1962 (HJD 2,437,971.594). This determination is based on 3 narrow-band photometric observations of Polaris by Williams (1966), transformed to the visual band, of which two were made on consecutive nights and the other 77 days later (19 pulsation cycles). Regrettably, no other useful photometric or RV measurements during this time have been identified in the literature, although it is possible they exist.

### 4.3. Pulsation Amplitude Variations

The oscillations of Polaris as measured photometrically or spectroscopically have the same shape (e.g., Klagyivik & Szabados 2009), and differ only by a phase shift, as noted in the previous section, and by a scale factor. Historical estimates of the pulsation amplitude based on brightness measurements have generally been more problematic to interpret. They are typically less precise (made visually for the oldest estimates), less homogeneous, and it is well known for Cepheids and similar variable stars that the brightness changes are smaller in the visible than in blue light (see, e.g., Stebbins 1946; Klagyivik & Szabados 2009). This makes comparisons difficult when the wavelength of the observation is not well known, leading to increased scatter (e.g., Arellano Ferro 1983a). We return to this below.

Measures of the radial velocity amplitude of the pulsations in Polaris are less ambiguous, but are not without their challenges. Because of the complex velocity fields in the atmospheres of Cepheids, in principle the measured velocity range can depend to some extent on the depth of formation of the spectral lines used to measure the RVs (Sasselov & Lester 1990), as well as on the measuring technique (see, e.g., Anderson 2018b, 2019, and references therein). These effects on the amplitude do not seem to be as overwhelming as in the case of brightness measurements, but should nevertheless be kept in mind. For the RV sources from the literature used here, the approximate wavelength ranges of the observations are listed in Table 1, when known.

RV amplitude changes were first examined by Roemer (1965), who concluded there was no obvious variation during the 60+ yr of Lick Observatory observations (1896–1958). Turner et al. (2005) added another 40 yr of amplitude measurements from other RV sources. Their Figure 6 displaying all spectroscopic and photometric measurements together shows considerable dispersion, but this is largely due to the photometric estimates, which are typically more uncertain. Figure 7 (top) is a graphical representation of our RV amplitude measurements from Table 2, covering 125 yr. As is customary in the Cepheid literature, we plot the full amplitude of the variation ( $2A_{\text{puls}}$ ), rather than the semiamplitude.

It appears to us that the Lick observations do suggest a very slight reduction in the amplitude up to 1958, in agreement with Turner et al. (2005), whereas Roemer (1965) chose to be more conservative. As mentioned earlier, Polaris seems to have been neglected by spectroscopists for the following two decades, during which there happened to be a sharp reduction in the pulsa-



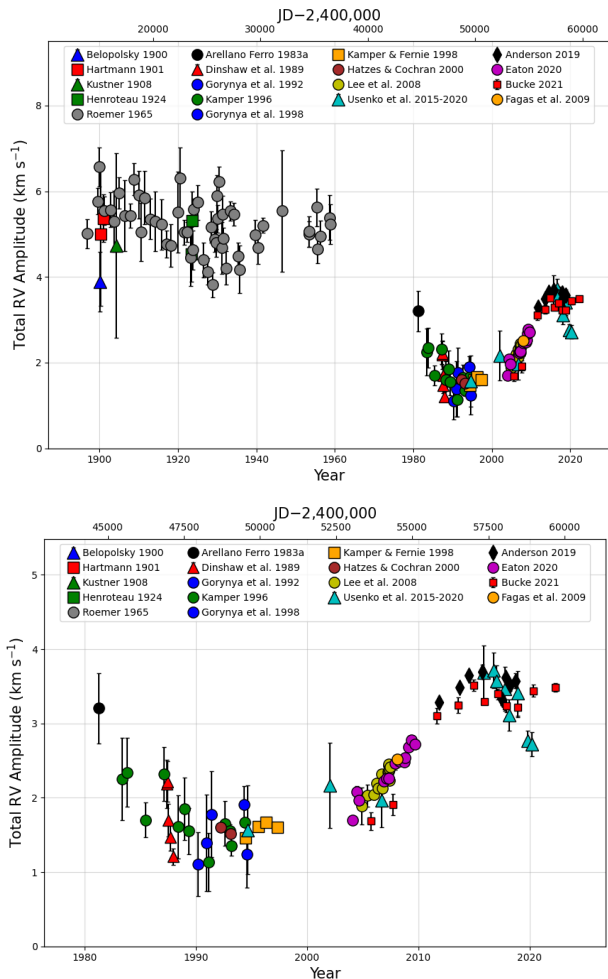


**Figure 7.** *Top:* Pulsation amplitude of Polaris (peak-to-peak) measured in this work from all available RV observations (Table 2). One additional measurement has been included, from the work of Fagas et al. (2009) (see the Appendix). *Bottom:* Enlargement showing the last four decades of amplitude measurements in closer detail.

tion amplitude. After 1980, the velocities from at least half a dozen independent observers showed the tail end of this amplitude decline, reaching a minimum peak-to-peak value of only  $\sim 1.5 \text{ km s}^{-1}$ . The amplitude then levelled off around 1990, and stayed low until about 1998. Beginning in 2002 it began to increase again, reaching a maximum of  $3.5 \text{ km s}^{-1}$  around 2015. The lower panel of Figure 7 zooms in on the last 40 yr of data. The three sources of measurements during the last decade (Anderson 2019, Bücke 2021, and Usenko and collaborators) display increased scatter. The measurements from the first two of these studies show little change in the amplitude after 2015, although they are at slightly different levels, whereas those of Usenko suggest another rather steep decline (Usenko et al. 2020). The reasons for these discrepancies are unclear. We note also that the amplitudes from the Bücke (2021) data (2005–2022) appear systematically lower by  $0.3$  or  $0.4 \text{ km s}^{-1}$  than other estimates obtained near in time. Finally, some of the scatter in Figure 7 may be real, as the RV range of the pulsations from cycle to cycle could be variable to some degree. And as pointed out earlier, differences in

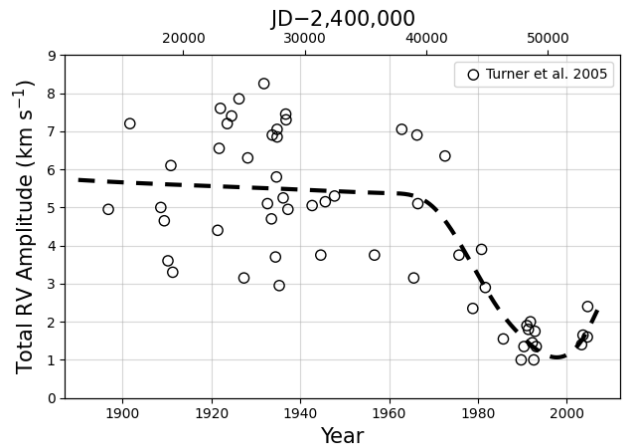


**Figure 8.** Photometric  $V$ -band estimates of the pulsation amplitude of Polaris by Turner et al. (2005), scaled up by a factor of 50 to match the peak-to-peak amplitude measurements from the RVs. A dashed line has been drawn by eye to mark the general trend, which is consistent with that shown in Figure 7 (top).

the spectral lines used, or in the techniques to measure the RVs, can also add scatter.

While there is a gap in the spectroscopic measures of the pulsation amplitude during the critical period between 1960 and 1980, a few photometric estimates do exist in this interval, although they exhibit considerable scatter, particularly before 1980. In Figure 8 we represent all light amplitude determinations by Turner et al. (2005), which the author measured in a uniform way and kindly provided to us. They are all presumed to correspond to the  $V$  band, and we have scaled them here so as to match the velocity amplitudes ( $\Delta RV = 2A_{\text{puls}}$ ) using  $\Delta RV = 50 \Delta V$ , where the coefficient of  $50 \text{ km s}^{-1} \text{ mag}^{-1}$  is the one adopted by Turner et al. (2005). The decline in the light amplitude during 1960–1980 is fairly obvious, and an approximate representation is shown by the dashed line drawn by eye. It is consistent with the trend observed in Figure 7 (top).

Much more precise measures of the peak-to-peak brightness amplitude have been obtained by several authors from the 2003–2011 SMEI observations (Bruntt et al. 2008; Švanda & Harmanec 2017; Anderson 2019). All three studies showed that the pulsation amplitude more than doubled during that period.<sup>7</sup> However, Anderson (2019) drew attention to a strong correlation between the growing photometric amplitude and the mean magnitude of Polaris measured from the same observations (his Figure 7). The correlation is in the sense that Polaris seemed to be getting fainter with time, by roughly  $0.08 \text{ mag}$  over that period. As this is unexpected, Anderson cautioned that the apparent dimming could be of instrumental origin, such as from a change in the detector’s non-linearity properties, and that this might also have resulted in a spurious change in the light amplitude. Radial velocity measurements are now available over the same period as the SMEI observations, and confirm, as mentioned earlier, that the pulsation amplitude was in fact increasing. We illustrate this in Figure 9, which compares the SMEI

<sup>7</sup> At the time of the Bruntt et al. (2008) paper, only about half of the SMEI data were available, but the amplitudes showed the same trend as the full dataset later analysed by others.

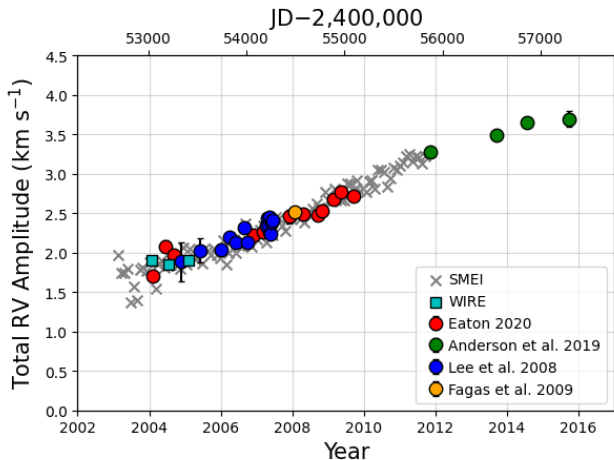


**Figure 9.** Comparison between the total pulsation amplitudes of Polaris from RVs and those based on the 2003–2011 SMEI photometry, as measured by Anderson (2019) and kindly provided by the author. The SMEI amplitudes have been scaled up here by a factor of 77 to match the peak-to-peak velocity amplitudes. This coefficient is different than in the visible because of the redder filter response of the photometric observations (roughly Johnson  $R$ ), but is similar to that found by Bruntt et al. (2008). The near perfect match of the slopes supports the accuracy of the photometric amplitudes. Three additional photometric amplitude measurements from the WIRE satellite are also shown. They were extracted from Figure 4 by Bruntt et al. (2008).

amplitudes from Anderson (2019) against those from the highest quality spectroscopic datasets over those years (Lee et al. 2008; Fagas et al. 2009; Anderson 2019; Eaton 2020). The agreement between these two completely independent ways of measuring the pulsation amplitude is excellent. In addition to supporting the accuracy of the SMEI amplitude measurements, this would also seem to lend credence to the finding by Anderson (2019) that the average brightness of Polaris was decreasing at the time (but see below).

Accurate measurements of the mean magnitude of Polaris over long periods of time are challenging, to say the least, and in that sense the SMEI observations are unique for their precision and continuity. We are not aware of any detailed study of the long-term evolution of its brightness, other than brief reports by Engle et al. (2004a,b, 2014). These authors claimed that Polaris seems to have become brighter in the last century by one or two tenths of a magnitude, and that examination of historical records going back to Ptolemy and Hipparchus suggest it may have been much fainter by a magnitude or more some 2000 years ago.<sup>8</sup> We note, however, that Neuhäuser et al. (2022) have expressed some reservations about the significance of the differences between the oldest measurements and current ones. Turner (2009) also doubted those claims, and concluded that the brightness of Polaris appears to have been constant at  $V \approx 2.00$  for the past century and a half.

## 5. DISCUSSION

The spectroscopic orbit of Polaris is a key ingredient for determining the dynamical masses of the components, as it provides the so-called mass function of

the binary, or equivalently, the minimum secondary mass  $M_{\text{Ab}} \sin i = (P/2\pi G)^{1/3} \sqrt{1 - e^2} K (M_{\text{Aa}} + M_{\text{Ab}})^{2/3}$ . In this expression, the mass sum on the right is obtained from the astrometric orbit and the parallax, through Kepler’s third law. The precision in the masses is currently limited by the astrometry, which has very sparse phase coverage from the five available HST observations, and in some cases sizeable uncertainties due to the difficulty of the measurements (Evans et al. 2008, 2018). Nevertheless, there is also some contribution from the uncertainty in the spectroscopic orbital elements. Table 7 compares our improved spectroscopic elements to others published previously. In earlier solutions, the contribution of the spectroscopy to the uncertainty in the masses was at the level of 1–3%, in most cases. By using twice the number of RV measurements now covering 4.3 cycles of the binary, the present work reduces this contribution by an order of magnitude. The dominant term in the mass error budget will then continue to come from the astrometry, particularly the inclination angle and the semimajor axis, until additional coverage of the orbit can be obtained.

The most recent dynamical mass determination for Polaris by Evans et al. (2018), giving  $3.45 \pm 0.75 M_{\odot}$  and  $1.63 \pm 0.49 M_{\odot}$  for the primary and secondary, respectively, relied on spectroscopic elements from previous work, which were held fixed. The elements  $P$ ,  $e$ , and  $\omega$  were adopted from Kamper (1996), while the time of periastron passage  $T_{\text{peri}}$  was taken from Wielen et al. (2000). Our improved results show subtle differences with those elements, particularly in the period and eccentricity (Table 7), which may have a non-negligible impact on the masses because the astrometric measurements only cover a small fraction of the orbit so far. However, given that the mass errors remain dominated by the astrometry, there is relatively little reward in repeating that determination at the present time. Further astrometric observations of Polaris are currently underway (see Evans et al. 2018), and may soon lead to significant improvements.

Up until the mid 1990s, there were differing opinions about the mode in which Polaris pulsates, some arguing for the fundamental mode, and others for the first or even second overtone. See, e.g., Evans et al. (2018), Bond et al. (2018), Engle et al. (2018), or Anderson (2018a) for summaries of those discussions. Much of the debate hinged on the uncertain distance of Polaris (and hence its radius and luminosity). A variety of methods have been used for that purpose, including trigonometric parallaxes from the ground (van Altena et al. 1995) and with HST (Bond et al. 2018), photometric parallaxes of Polaris B (Turner 1977; Turner et al. 2013), absolute magnitude estimates based on spectroscopic line ratios calibrated against supergiants with well-established luminosities (Turner et al. 2013), and others. The distance issue was eventually settled by the Hipparcos mission, although not without further debate (see Turner et al. 2013; van Leeuwen 2013; Bond et al. 2018). The Gaia mission finally confirmed the accuracy of the Hipparcos result by measuring the parallax of Polaris B, and increased the precision by about a factor of ten. Polaris is now considered to be a first overtone pulsator (e.g., Anderson 2018a, 2019), consistent with its small amplitude, symmetric light curve, and its rapid rate of period

<sup>8</sup> See also the popular account in *Sky & Telescope*, Vol. 137, No. 3, p. 14 (March 2019).

**Table 7**  
Spectroscopic Orbital Solutions for Polaris

Source	$P$ (yr)	$\gamma$ (km s <sup>-1</sup> )	$K$ (km s <sup>-1</sup> )	$e$	$\omega$ (degree)	$T_{\text{peri}}$ (yr)
Moore (1929)	29.6	-17.4	4.05	0.63	332.0	1899.5
Gerasimovic (1936)	29.6 (assumed)	-16.5	4.35	0.50	315.8	1899.8
Roemer (1965)	30.46 ± 0.15	-16.41	4.09 ± 0.15	0.639 ± 0.018	307.2 ± 2.7	1928.48 ± 0.12
Kamper et al. (1984)	30.03 ± 0.07	-16.31 ± 0.04	4.01 ± 0.06	0.655 ± 0.013	307.2 ± 1.1	1929.86 ± 0.11
Kamper (1996)	29.59 ± 0.02	-16.42 ± 0.03	3.72 ± 0.03	0.608 ± 0.005	303.01 ± 0.75	1928.48 ± 0.08
Turner (2009)	29.71 ± 0.09	-15.90 ± 0.06	4.41 ± 0.07	0.543 ± 0.010	309.6 ± 0.7	1928.57 ± 0.06
Turner (2009)	29.80 ± 0.05	-15.87 ± 0.05	4.23 ± 0.07	0.52 ± 0.01	301 ± 2	1928.50 ± 0.12
Anderson (2019)	29.32 ± 0.11	-15.387 ± 0.040	3.768 ± 0.073	0.620 ± 0.008	307.2 ± 2.5	2016.91 ± 0.10
Usenko et al. (2020)	29.25 ± 0.03	-16.61 ± 0.12	3.93 ± 0.12	0.633 ± 0.044	302.5 ± 2.7	1987.22 ± 0.10
Bücke (2021)	29.31 ± 0.07	-17.1 ± 0.4	3.74 ± 0.06	0.574 ± 0.010	300.7 ± 3.0	2016.77 ± 0.10
This work	29.4330 ± 0.0079	-16.084 ± 0.025	3.7409 ± 0.0075	0.6195 ± 0.0015	302.04 ± 0.34	2016.801 ± 0.011

change, which in this type of objects is about an order of magnitude faster than seen in Cepheids that are pulsating in the fundamental mode (e.g., Szabados 1983). Secular period changes in Cepheids are not uncommon (see, e.g., Csörnyei et al. 2022). A period increase is indicative of evolution toward cooler temperatures, and for fundamental mode pulsators, the rates are broadly in agreement with predictions from stellar evolution models.

Except for a brief interruption in the mid 1960s, the monotonic increase in the pulsation period of Polaris until about 2005, at a rapid rate of  $\sim 4.5$  s yr<sup>-1</sup>, was considered a sign that the star was evolving to the right in the H-R diagram (e.g., Turner et al. 2006), and was about to exit the instability strip. This idea was driven in part by the declining pulsation amplitude, and by the belief that Polaris was near the red edge of the instability strip, whereas revisions in the distance locate it closer to the blue edge (see, e.g., Anderson 2019; Ripepi et al. 2021). The fact that the period is now becoming shorter also complicates this picture, as evolution is expected to proceed only in one direction. The glitch circa 1965 has defied explanation as well, although Turner et al. (2005) have speculated that it could be accounted for by a sudden increase in the mass of the Cepheid, such as by the ingestion of a large ( $\sim 7 M_{\text{Jup}}$ ) planet. Evans et al. (2002, 2018) have argued that for overtone pulsators like Polaris, period changes are not necessarily caused by evolution across the instability strip. Instead, they may simply reflect more erratic behaviour related to the pulsation itself, which is still poorly understood. The irregular fluctuations in the pulsation amplitude would seem to support that notion.

It has been proposed that some of these irregular changes in the properties of the pulsation may be related to the binarity of Polaris (e.g., Dinshaw et al. 1989; Usenko et al. 2020). Discontinuities in the  $O-C$  diagram, such as the one in the mid 1960s, have long been seen also in other Cepheids (e.g., Szabados 1989, 1991; Csörnyei et al. 2022), and are sometimes referred to as phase jumps or phase slips. Szabados (1992) pointed out that such features appear to be common in binary Cepheids, more so than in Cepheids that are single, and that they seem to repeat with a cycle length similar to the period of the binary, or multiples of it. They would be explained by the perturbing influence of the companion on the upper layers of the atmosphere of the Cepheid, where the pulsations take place, during or near the times of periastron

passage.

The separation between Polaris and its 30 yr companion at periastron is approximately 6.2 au. This follows from the angular semimajor axis of the astrometric orbit by Evans et al. (2018) ( $a = 0''.12$ ), our value for the eccentricity ( $e = 0.62$ ), and the parallax of Polaris B from the Gaia mission. The latest Gaia data release (DR3; Gaia Collaboration et al. 2022) puts the parallax at  $\pi_{\text{Gaia}} = 7.305$  mas, including a zeropoint correction by Lindegren et al. (2021). Polaris has a measured angular diameter of  $3.123 \pm 0.008$  mas (Mérand et al. 2006), which corresponds to a physical radius of  $46 R_{\odot}$  at the distance from Gaia (137 pc). The periastron separation is therefore about 29 times the radius of the Cepheid.

In Figure 10 we reproduce the pulsation velocity amplitudes and instantaneous pulsation period of Polaris from earlier figures. The dashed lines mark the periastron passages according to our updated spectroscopic orbit. There are intriguing coincidences between features in these diagrams and the dates of minimum separation of the binary. In the top panel, the 1957 periastron came just before the sharp drop in the RV amplitude that took place between 1960 and 1980. The exact date at which this decline began is difficult to pinpoint due to a lack of measurements. It may have started a few years into the 1960–1980 gap, as Figure 8 might suggest. It would not be surprising if the period jump in the lower panel coincided with that instant, as it also occurred just a few years after closest approach in 1957. The following periastron passage, in 1987, came just before the RV amplitudes reached their lowest point and reversed course. At about the same time, there is a slight change in the slope of the curve representing the evolution of the pulsation period, although the reality of this feature is unclear as it depends to some extent on the smoothing applied to the curve. The most recent periastron passage of 2016 occurred just as the RV amplitudes appeared to reach a peak. At about this time, or slightly earlier, the period of Polaris began to decrease.

Earlier periastron passages appear less remarkable, as the data are either sparser or of lesser quality. There is a hint that the 1928 passage may coincide with a downward kink in the distribution of velocity amplitudes, although we cannot be certain given the precision of the data. The passage of 1899 occurred near an inflection point in the period diagram, but again, the data here are scarce, particularly before 1900 (Figure 6, top).

Taken together, these instances are highly suggestive of

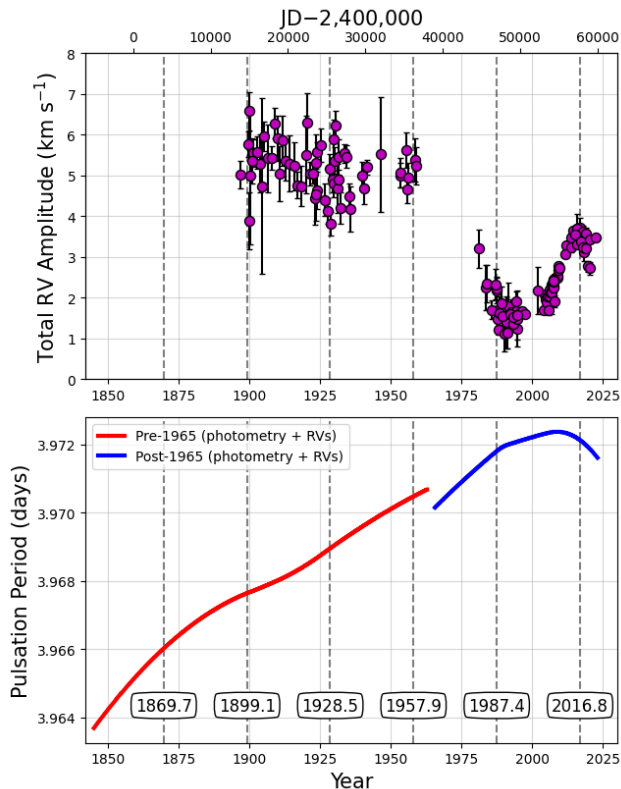


**Figure 10.** RV amplitude of Polaris (top) and instantaneous pulsation period (bottom) as a function of time (from Figures 6 and 7), with periastron passages marked with dashed lines and labelled.

a cause-and-effect connection between changes in the pulsation behaviour of Polaris and the recurring approaches of the companion every 30 yr. The implication would be that the upper atmosphere of the Cepheid is undergoing enhanced, forced tidal perturbations induced by the secondary. Such tidal forcing in eccentric binaries is also seen in a very different context, in the class of main-sequence objects known as “heartbeat stars” (see, e.g., Welsh et al. 2011). In these systems, which are typically very eccentric, each periastron passage is responsible for exciting a rich set of stellar pulsations with a large number of modes, giving the lightcurves their characteristic appearance of an electrocardiogram.

In overtone Cepheid pulsators such as Polaris, Evans et al. (2002) have argued that the oscillations react in a more unstable way than in fundamental mode pulsators to small changes driven by stellar evolution, as mentioned earlier. It would therefore not be surprising if they reacted in a similar manner to the periodic approach of the companion.

## 6. CONCLUSIONS

In this work, we have taken advantage of the large body of RV measurements in the literature of the past 125 yr to revisit the pulsation properties of Polaris, and

to improve its spectroscopic orbit. All of the spectroscopic elements now have uncertainties that are several times smaller than before, and should serve as the basis for a more accurate mass determination for the Cepheid, once additional astrometric observations along the 30 yr orbit are secured.

Notwithstanding its long observational history, Polaris continues to be an object of great astrophysical interest. Our RV analysis has provided clear evidence confirming earlier indications that the pulsation period is now becoming shorter, starting around the year 2010. This change in direction, compared to the prevailing trend during most of the 20th century, is inconsistent with the previous interpretation that the period change reflected rapid evolution across the instability strip.

Our analysis has also enabled us to more precisely map changes in the RV amplitude of the pulsation since 1900. We have shown that after the sharp  $\sim 1960$ – $1990$  decline, and the almost equally rapid recovery thereafter, the amplitude stopped increasing roughly around 2016. It may have started to decrease again, although this needs to be confirmed with further measurements in the coming years.

These irregular period and amplitude changes seem consistent with the claim of Evans et al. (2002, 2018) that the oscillations in overtone pulsators such as Polaris are more unsteady than those in fundamental mode pulsators, and sensitive to small evolutionary changes. Interestingly, we have found that these changes appear to have a connection to the binarity of Polaris, always occurring near the times of periastron passage in the 30 yr orbit, at least so far. This could be the result of forced tidal perturbations by the companion, and would support the idea by Evans and collaborators that the pulsations are easily influenced by other effects, in this case an external force.

We are grateful to D. Turner, the referee, for sharing the spreadsheets with his original data compilations and reductions, and for helpful comments on the original manuscript. We also thank B.-C. Lee and R. Bücke for providing their unpublished radial velocities for our analysis, and R. Anderson for sending his photometric amplitude measurements based on the SMEI observations.

This research has made use of the SIMBAD and VizieR databases, operated at the CDS, Strasbourg, France, and of NASA’s Astrophysics Data System Abstract Service. The computational resources used for this research include the Smithsonian High Performance Cluster (SI/HPC), Smithsonian Institution (<https://doi.org/10.25572/SIHPC>).

## 7. DATA AVAILABILITY

The data underlying this article are available in the article and in its online supplementary material.

## APPENDIX

### HISTORICAL RADIAL VELOCITIES

Here we provide details of the various sources of radial velocity measurements for Polaris listed in Table 1 of the main text, in the order in which they appear there. We describe only the original sources, except where the velocities have been adjusted or otherwise superseded in subsequent publications.

**Vogel (1895):** These are the earliest two radial velocity measurements reported for Polaris, obtained at the Potsdam Observatory (Germany) in November and December of 1888. They were originally published in units of German geographical miles ( $7.42 \text{ km s}^{-1}$ ), and are too poor to be of use here.

**Roemer (1965):** The longest and most complete series of measurements, consisting of 1180 velocities made with the Mills spectrograph on the 36-inch refractor at the Lick Observatory (California, USA) between 1898 and 1958. These data cover more than two cycles of the binary, including three periastron passages, and are valuable for improving the orbital period when combined with modern observations. We have assigned them initial uncertainties of  $0.5 \text{ km s}^{-1}$  each. In the course of using these measurements, we noticed a systematic shift in the residuals from a preliminary orbital solution between the velocities before and after about 1920. The ones before appear consistently more negative by about  $0.8 \text{ km s}^{-1}$ . While the reasons for this are unclear, the original publication indicates that, prior to that date, no account was taken of the flexure of the telescope tube, whereas the data taken afterwards did include corrections for that effect. For the present analysis, we have chosen to adjust the older velocities by  $+0.8 \text{ km s}^{-1}$ , to place them approximately on the same footing as the more recent Lick data. The original publication also mentioned a hint of a semiregular variation in the observations up to 1920, with a period of 6–8 yr and a total amplitude of about  $1 \text{ km s}^{-1}$ . However, as this is not seen clearly in subsequent data from the same series, we have not considered it further. The study reported the first detailed determination of the spectroscopic orbital elements, which had previously only been published by others without associated uncertainties.

**Frost (1899):** Three observations from the Yerkes Observatory (Wisconsin, USA) in August and September of 1899. They show clear variability due to the pulsations, but are too few and too scattered to be useful. A fourth observation was mentioned to have been taken, but the results were never published, as far as we can tell.

**Bélopolsky (1900):** These 17 velocity measurements from the Potsdam Observatory were made between November of 1899 and March of 1900, occasionally more than once per night. They were gathered at a time when there was little change in the orbital velocity of Polaris, which was at its maximum. They are therefore of little use here for constraining the orbit, because of the need to allow for an offset to account for the unknown velocity zeropoint relative to other measurements. Nevertheless, we have used them to obtain a measurement of the pulsation amplitude and a time of minimum velocity, to constrain changes in the orbital period. Measurement uncertainties were assumed here to be  $1.5 \text{ km s}^{-1}$ , based on the intra-night scatter.

**Hartmann (1901):** This series of 35 measurements between March of 1900 and January of 1901 was also gathered at the Potsdam Observatory. Individual uncertainties as reported in the publication range from  $1.8 \text{ km s}^{-1}$  for the earlier measurements to  $0.7 \text{ km s}^{-1}$  for the more recent ones.

**Küstner (1908):** Seven velocity observations from the Bonn Observatory (Germany) were made in July of 1903 and May–June of 1905, at a time when the orbital velocity was changing significantly. Typical uncertainties as reported in the paper are  $0.95 \text{ km s}^{-1}$ .

**Abt (1970):** The catalogue of Mount Wilson Observatory (California, USA) radial velocity measurements lists only 3 observations made with different instrumental dispersions, two on the same night in 1916, and the other in 1932. They are not useful for the present work.

**Henroteau (1924):** This source contains 58 measurements of the RV made at the Dominion Observatory (Ottawa, Canada) between April and September of 1923. The orbital velocity of Polaris was not changing significantly during this time, so the observations do not constrain the orbit for the same reason mentioned earlier for the Bélopolsky (1900) velocities. However, they do provide useful measurements of the pulsation amplitude and time of minimum velocity.

**Schmidt (1974):** These authors reported only a single RV measurement of Polaris, obtained in 1971 at the Kitt Peak Observatory (Arizona, USA). It is one of the very few measurements we have located in the poorly observed 20 yr period between 1960 and 1980, but it does not provide any useful information for this work.

**Wilson et al. (1989):** These three RVs of Polaris from 1977, obtained at the McDonald Observatory (Texas, USA), are the only others found between 1960–1980, but are also too few to be useful. They cover less than one pulsation cycle.

**Arellano Ferro (1983a):** This series of 35 RV measurements was made at the David Dunlap Observatory and the Dominion Astrophysical Observatory (DAO), both in Canada, from July of 1980 to January of 1982. The uncertainties were adopted as published, after a conversion from probable errors to mean errors. All but 6 of these measurements were later republished by Kamper (1996), along with many others also from the David Dunlap Observatory. In that publication, a  $+0.5 \text{ km s}^{-1}$  offset was applied to the Arellano Ferro (1983a) RVs to bring them onto the same scale as the rest of those measurements. For the present work we have applied the same  $+0.5 \text{ km s}^{-1}$  offset to the Arellano Ferro (1983a) velocities, including the 6 not listed by Kamper, so that they may be considered jointly with the Kamper velocities and avoid adding another free parameter to our analysis that would otherwise be needed to account for the difference in the zeropoints.

**Beavers & Eitter (1986):** This work reports a single RV measurement made in 1980 at the Erwin W. Fick Observatory (Iowa, USA). We have ignored for the present work.

**Kamper et al. (1984):** This is a small subset of the velocities published later by Kamper (1996), in which minor adjustments were made to the measurements. We therefore consider them to have been superseded by the latter publication (see below).

**Kamper (1996):** This extensive series of 421 observations at the David Dunlap Observatory (1983–1995) relied on a variety of observational and measurement techniques, beginning with photographic plates at several dispersions until early 1990, then using a Reticon detector, and finally replacing it with a CCD and analysing the spectra with cross-correlation methods. These changes in instrumentation and processing made it difficult to place all of the velocities onto a consistent system, despite the use of IAU radial velocity standards in some intervals, or of the telluric oxygen band at 6300 Å as the velocity reference, for the more recent CCD data. As a result, the author cautioned that the earlier measurements that did not use the oxygen band may be subject to systematic errors of comparable size to the frame-to-frame scatter. Clear evidence of this was shown in Figure 5 by Anderson (2019), in which the raw velocities from the Reticon observations are seen to be systematically higher than other measurements taken near in time, by roughly  $1 \text{ km s}^{-1}$ . A similar offset is seen for observations during the 1992 July–August run, in the same direction, and for an entire campaign during 1991 July–September in which a fibre link was used. In this latter case the shift appears to be about  $1 \text{ km s}^{-1}$  in the opposite direction (i.e., lower than other contemporaneous velocities). With some hesitation, we have chosen here to adjust the measurements in those intervals by the amounts indicated, in an attempt to remove these rather obvious shifts and make the entire dataset more homogeneous. A few other intervals with smaller systematic deviations are discernible, but we have refrained from further tinkering with the data and simply accept those instances as contributing to the natural scatter. As mentioned earlier, Kamper (1996) list all but 6 of the Arellano Ferro (1983a) velocities, which we will not consider as part of this group. Additionally, it lists 79 observations after 1994 April that have been superseded by a later publication (Kamper & Fernie 1998), in which thermal effects were corrected. For the present work we will consider this dataset to contain only the  $421 - 35 - 79 = 307$  measurements that are not reported by either Arellano Ferro (1983a) or Kamper & Fernie (1998). This collection of observations is important because it has complete coverage of the periastron passage of 1987, from velocity minimum to maximum, and part of the way down again. Uncertainties for the individual observations depend on the technique, and from our best understanding of the description, they range between about  $0.5 \text{ km s}^{-1}$  for the photographic measurements and  $0.15 \text{ km s}^{-1}$  for the more recent observations recorded in digital form. These observations were used by Kamper, both separately and in combination with the Lick observations of Roemer (1965), to derive the elements of the spectroscopic binary orbit that have been most commonly used in subsequent investigations of Polaris.

**Dinshaw et al. (1989):** These authors reported 175 velocities for Polaris, made between 1987 and 1988 at the University of British Columbia’s Wreck Beach Observatory (Canada). The uncertainties have been adopted here as described in that work, with those of measurements that are the mean from 2–3 spectra being reduced by  $\sqrt{2}$ . A slight complication with these observations is that, rather than being absolute, they were measured relative to the first observation. More importantly, the RVs show a long-term trend that the authors attributed mostly to orbital motion of the binary, although from their description there may also be a component due to mechanical flexure of the telescope tube. This long-term trend is shown in their Figure 2, together with a second-order polynomial approximation that they then subtracted from the relative velocities. The polynomial coefficients were not reported, and the individual velocity measurements listed in their paper are only those after removal of that long-term trend. For our analysis, we digitised the figure to extract the coefficients of the quadratic fit, and then removed it from the listed measurements in order to recover the relative velocities. In addition to the RV changes due to the 4-day pulsation, Dinshaw et al. (1989) reported the detection of a signal with a 45 day period and a total amplitude of about  $1 \text{ km s}^{-1}$ . Prior to using these data for our orbital analysis, we subtracted this variation out, as described in the main text.

**Sasselov & Lester (1990):** These authors reported two RV measurements made at infrared wavelengths ( $1.1 \mu\text{m}$ ) with the Fourier transform spectrometer at the Canada-France-Hawaii Telescope (Hawaii, USA). They were obtained 4 nights apart in September/October of 1988, but are not useful for our purposes.

**Gorynya et al. (1992):** This work reports 32 RVs made in 1990 and 1991 at the Shternberg State Astronomical Institute in Moscow (Russia), with a CORAVEL-type spectrometer delivering typical precisions of  $0.3 \text{ km s}^{-1}$ .

**Garnavich et al. (1993):** This short note reports only that Polaris was monitored beginning in 1992 with a hydrogen fluoride gas absorption cell on the DAO coude spectrograph, achieving internal velocity precisions of tens of  $\text{m s}^{-1}$  (higher than any of the previous velocities). As far as we are aware, the individual measurements, which appear to have been made over at least a year, were never published or discussed in the literature, and are not available.

**Hatzes & Cochran (2000):** This series of 42 high precision velocity measurements was made in 1992–1993 on the 2.1m telescope at the McDonald Observatory (Texas, USA), using an iodine gas absorption cell as the reference. These are again relative velocities, with an internal precision estimated by the authors to be  $50\text{--}70 \text{ m s}^{-1}$ . We adopted the higher value for our work. After removal of the pulsation variation, a frequency analysis by Hatzes & Cochran (2000) revealed a 40-day periodicity in the residuals, similar to the signal found by Dinshaw et al. (1989), but with a smaller total amplitude of about  $0.4 \text{ km s}^{-1}$ . As in that case, we have removed this variability before using these relative velocities to constrain the binary orbit.

**Gorynya et al. (1998):** These authors reported an additional 40 velocities of Polaris made in 1994, with the same

instrumentation as their 1992 paper (see above). We consider them together with those measurements for the purpose of updating the spectroscopic orbit. We adopted the velocity uncertainties as published.

**Usenko et al. (2015):** A total of 56 velocities were made with three different telescope/instrument combinations in the US and in Russia, between 1994 and 2009. The 2003–2004 subset of these measurements shows little coherence, with the 4-day pulsation variability not clearly present. The author pointed out the unusual behaviour of the  $H\alpha$  line during these years (asymmetries, and a significant RV difference between the core of the  $H\alpha$  line and the RVs from metal lines). While this could indicate a real phenomenon in the atmosphere of Polaris, much higher quality measurements during 2004 by Eaton (2020), which we describe below, appear completely normal and show the pulsations clearly. We are inclined to believe that Usenko’s 2003–2004 measurements may have been impacted by significant fluctuations in the velocity zero point, and we have elected not to use them here. The remainder of their observations appear to be unaffected.

**Kamper & Fernie (1998):** This dataset consists of 212 RV measurements of Polaris from the David Dunlap Observatory, made between 1995 and 1997. Uncertainties were adopted as published. Of these measurements, 79 had been reported earlier by Kamper (1996), but were corrected here for thermal effects. All of these velocities were measured relative to the first one, and the listing of the individual values in Table 1 of Kamper & Fernie (1998) has the orbital motion subtracted out, using the elements published by Kamper (1996). For our purposes, we have added the orbital motion back in, using those same elements.

**Eaton (2020):** This is the second most extensive set of RVs for Polaris, after the Lick series. The 679 observations, of excellent quality (typical internal errors of  $0.11 \text{ km s}^{-1}$ ), were obtained between 2003 and 2009 with the Tennessee State University’s 2m Automatic Spectroscopic Telescope at the Fairborn Observatory (Arizona, USA). A subset of these measurements was used by Bruntt et al. (2008) in a study of changes in the pulsation period and amplitude. The remaining observations appear not to have been used until now.

**Lee et al. (2008):** This is another series of very precise relative velocity measurements made with an iodine absorption cell, using a high-resolution echelle spectrograph on the 1.8m telescope at the Bohyunsan Optical Astronomy Observatory (Korea). Although the RVs were not listed in the paper, the lead author was kind enough to give us access to the 265 measurements, which have typical formal uncertainties of  $10\text{--}20 \text{ m s}^{-1}$ . As shown in Figure 1 by those authors, the velocities display a clear trend due to the orbital motion of the binary. In addition to the well-known pulsation, they reported an additional  $\sim 120$  day periodicity with a peak-to-peak amplitude just under  $0.3 \text{ km s}^{-1}$ . We have removed this signal in preparation for use of these velocities for our orbital analysis, as described in the main text.

**Bücke (2021):** As with the previous dataset, these RVs for Polaris have not been published, but were made available to us by the author, Roland Bücke, who is an amateur astronomer based in Germany.<sup>9</sup> This is an untapped series of 296 observations made between 2005 and 2023, using a backyard 8-inch and later an 18-inch Dobsonian telescope, coupled with an  $R \approx 3500$  spectrograph via an optical fibre. The measurements are relative to the first observation, and span more than 60% of the 30 yr orbital cycle. They provide dense coverage of the phases between minimum and maximum radial velocity, including the latest periastron passage of 2016. The spectrograph is not thermally controlled, and the velocities display obvious seasonal changes that we have removed with a spline approximation (after subtracting the pulsation and orbital variations). Further details are given in the main text. Initial uncertainties for our analysis were adopted as supplied by the author.

**Fagas et al. (2009):** This is another dataset that appears to have never been published. The scant information available indicates that 330 spectra were obtained over a 7 month period (2007 December to 2008 July), with the 0.4m Poznan Spectroscopic Telescope (Poland) and a fibre-fed spectrograph. While the original data are not available to us, the authors reported a useful measurement of the total velocity amplitude of  $2A_{\text{puls}} = 2.52 \pm 0.03 \text{ km s}^{-1}$ , from the first four months of their observations. This value is consistent with others obtained during the same period (see the main text).

**De Medeiros et al. (2014):** The brief report by these authors indicated that 13 RV measurements of Polaris were made over a period of 6098 days using the CORAVEL instrument on the 1.93m telescope at the Haute-Provence Observatory (France). They were never published, but in any case, because of the sparseness of the observations, the measures are unlikely to be of much help for our analysis.

**Anderson (2019):** This is a high-quality set of 161 observations, obtained between 2011 and 2018 with the Hermes spectrograph on the 1.2m Mercator telescope on the Roque de los Muchachos Observatory (La Palma, Canary Island, Spain). The velocities are on an absolute scale, and have formal uncertainties of  $15 \text{ m s}^{-1}$ , which reflect only the short-term precision. A template matching procedure designed to remove the pulsation variations was carried out by Anderson, and applied to the Hermes observations and those of Kamper (1996) to derive a new set of orbital elements for the binary.

**Usenko et al. (2016, 2017, 2018, 2020):** These studies continued the RV monitoring of Polaris initiated by Usenko et al. (2015), but now mostly with the 0.81m telescope at the Three College Observatory (North Carolina, USA), and

<sup>9</sup> See <http://astro.buecke.de/index.html>

occasionally with a 0.6m telescope at the Kernesville Observatory, also in North Carolina. Collectively, the observations span the interval 2015–2020 and cover the recent periastron passage of 2016. A total of 21, 49, 67, and 53 velocity measurements were reported in each of these four studies, respectively. In the final paper of this series, the authors derived an updated spectroscopic orbit combining their own observations with seasonal averages from Anderson (2019) and Roemer (1965).

## REFERENCES

- Abt, H. A. 1970, *ApJS*, 19, 387
- Anderson, R. I. 2018a, *A&A*, 611, L7
- Anderson, R. I. 2018b, The RR Lyrae 2017 Conference. Revival of the Classical Pulsators: from Galactic Structure to Stellar Interior Diagnostics, Proceedings of the Polish Astronomical Society, Vol. 6. Edited by R. Smolec, K. Kinemuchi, and R.I. Anderson, p. 193
- Anderson, R. I. 2019, *A&A*, 623, A146
- Arellano Ferro, A. 1983a, *ApJ*, 274, 755
- Arellano Ferro, A. 1983b, Ph.D. thesis, University of Toronto, Canada
- Beavers, W. I. & Eitter, J. J. 1986, *ApJS*, 62, 147
- Bélopolsky, A. 1900, *Astronomische Nachrichten*, 152, 199
- Berdnikov, L. N. & Pastukhova, E. N. 1995, *Astronomy Letters*, 21, 369
- Bond, H. E., Nelan, E. P., Remage Evans, N., et al. 2018, *ApJ*, 853, 55
- Bono, G., Gieren, W. P., Marconi, M., et al. 2001, *ApJ*, 563, 319
- Brown, C. F. & Bochonko, D. R. 1994, *PASP*, 106, 964
- Bruntt, H., Evans, N. R., Stello, D., et al. 2008, *ApJ*, 683, 433
- Bücke, R. 2021, *BAV Magazine Spectroscopy* 09/2021, 9, 43
- Campbell, W. W. 1899, *PASP*, 11, 195
- Csörnyei, G., Szabados, L., Molnár, L., et al. 2022, *MNRAS*, 511, 2125
- De Medeiros, J. R., Alves, S., Udry, S., et al. 2014, *A&A*, 561, A126
- Dinshaw, N., Matthews, J. M., Walker, G. A. H., et al. 1989, *AJ*, 98, 2249
- Eaton, J. A. 2020, *Journal of the American Association of Variable Star Observers*, 48, 91
- Efremov, Yu. N. 1975, *Pulsating Stars*, ed. B. V. Kukarkin (John Wiley & Sons, New York), 42
- Engle, S. G., Guinan, E. F., & Koch, R. H. 2004, *BAAS*, 36, 744
- Engle, S. G., Guinan, E. F., & Kim, C.-W. 2004, *BAAS*, 37, 378
- Engle, S. G., Guinan, E. F., & Harmanec, P. 2018, *Research Notes of the American Astronomical Society*, 2, 126
- Engle, S. G., Guinan, E. F., Harmanec, P., et al. 2014, *BAAS*, 46, #156.18
- Evans, N. R., Karovska, M., Bond, H. E., et al. 2018, *ApJ*, 863, 187
- Evans, N. R., Sasselov, D. D., & Short, C. I. 2002, *ApJ*, 567, 1121
- Evans, N. R., Schaefer, G. H., Bond, H. E., et al. 2008, *AJ*, 136, 1137
- Fagas, M., Baranowski, R., Bartczak, P., et al. 2009, *Communications in Asteroseismology*, 159, 48
- Feast, M. W. & Catchpole, R. M. 1997, *MNRAS*, 286, L1
- Fernie, J. D., Kamper, K. W., & Seager, S. 1993, *ApJ*, 416, 820
- Foreman-Mackey, D., Hogg, D. W., Lang, D., & Goodman, J. 2013, *PASP*, 125, 306
- Frost, E. B. 1899, *ApJ*, 10, 184
- Gaia Collaboration, Brown, A. G. A., Vallenari, A., et al. 2018, *A&A*, 616, A1
- Gaia Collaboration, Vallenari, A., Brown, A. G. A., et al. 2022, *arXiv:2208.00211*
- Garnavich, P., Yang, S., Matthews, J. M., et al. 1993, *JRASC*, 87, 187
- Gelman, A. & Rubin, D. B. 1992, *Statistical Science*, 7, 457
- Gerasimovic, B. P. 1924, *AJ*, 35, 181
- Gerasimovic, B. P. 1936, *ApJ*, 84, 229
- Gorynya, N. A., Irmambetova, T. R., Rastorgouev, A. S., et al. 1992, *Soviet Astronomy Letters*, 18, 316
- Gorynya, N. A., Samus', N. N., Sachkov, M. E., et al. 1998, *Astronomy Letters*, 24, 815
- Hartmann, J. 1901, *ApJ*, 14, 52
- Hatzes, A. P. & Cochran, W. D. 2000, *AJ*, 120, 979
- Henroteau, F. 1924, *Publications of the Dominion Observatory Ottawa*, 9, 1
- Herschel, W. & Watson, D. 1782, *Philosophical Transactions of the Royal Society of London Series I*, 72, 112
- Kamper, K. W. 1996, *JRASC*, 90, 140
- Kamper, K. W., Evans, N. R., & Lyons, R. W. 1984, *JRASC*, 78, 173
- Kamper, K. W. & Fernie, J. D. 1998, *AJ*, 116, 936
- Klagyivik, P. & Szabados, L. 2009, *A&A*, 504, 959
- Küstner, F. 1908, *ApJ*, 27, 301
- Lee, B.-C., Mkrtychian, D. E., Han, I., et al. 2008, *AJ*, 135, 2240
- Lindegren, L., Bastian, U., Biermann, M., et al. 2021, *A&A*, 649, A4
- Mérand, A., Kervella, P., Coudé du Foresto, V., et al. 2006, *A&A*, 453, 155
- Moore, J. H. 1929, *PASP*, 41, 56
- Neilson, H. R., Cantiello, M., & Langer, N. 2011, *A&A*, 529, L9
- Neilson, H. R., Engle, S. G., Guinan, E., et al. 2012, *ApJ*, 745, L32
- Neuhäuser, R., Torres, G., Mugrauer, M., et al. 2022, *MNRAS*, 516, 693
- Ricker, G. R., Winn, J. N., Vanderspek, R., et al. 2015, *Journal of Astronomical Telescopes, Instruments, and Systems*, 1, 014003. doi:10.1117/1.JATIS.1.1.014003
- Ripepi, V., Catanzaro, G., Molnár, L., et al. 2021, *A&A*, 647, A111
- Roemer, E. 1965, *ApJ*, 141, 1415
- Sasselov, D. D. & Lester, J. B. 1990, *ApJ*, 362, 333
- Schmidt, E. G. 1974, *MNRAS*, 167, 613
- Spreckley, S. A. & Stevens, I. R. 2008, *MNRAS*, 388, 1239
- Stebbins, J. 1946, *ApJ*, 103, 108
- Švanda, M. & Harmanec, P. 2017, *Research Notes of the American Astronomical Society*, 1, 39
- Szabados, L. 1983, *Ap&SS*, 96, 185
- Szabados, L. 1991, *Communications of the Konkoly Observatory Hungary*, 96, 123
- Szabados, L. 1989, *Communications of the Konkoly Observatory Hungary*, 94, 1
- Szabados, L. 1992, *IAU Colloq.* 135, *Complementary Approaches to Double and Multiple Star Research*, ASP Conf. Ser., eds. H. A. McAlister and W. I. Hartkopf (San Francisco:ASP), 32, 255
- Turner, D. G. 1977, *PASP*, 89, 550
- Turner, D. G. 2009, *Stellar Pulsation: Challenges for Theory and Observation*, AIP Conf. Proc., eds. J. A. Guzik & P. A. Bradley (American Institute of Physics: Melville, NY), 1170, 59
- Turner, D. G., Abdel-Sabour Abdel-Latif, M., & Berdnikov, L. N. 2006, *PASP*, 118, 410
- Turner, D. G., Kovtyukh, V. V., Usenko, I. A., et al. 2013, *ApJ*, 762, L8
- Turner, D. G., Majaess, D. J., Lane, D. J., et al. 2010, *Odessa Astronomical Publications*, 23, 125
- Turner, D. G., Savoy, J., Derrah, J., et al. 2005, *PASP*, 117, 207
- Usenko, I. A., Kovtyukh, V. V., Miroshnichenko, A. S., et al. 2016, *Odessa Astronomical Publications*, 29, 100
- Usenko, I. A., Kovtyukh, V. V., Miroshnichenko, A. S., et al. 2017, *Odessa Astronomical Publications*, 30, 146
- Usenko, I. A., Kovtyukh, V. V., Miroshnichenko, A. S., et al. 2018, *MNRAS*, 481, L115
- Usenko, I. A., Miroshnichenko, A. S., Danford, S., et al. 2020, *Odessa Astronomical Publications*, 33, 65
- Usenko, I. A., Miroshnichenko, A. S., Klochkova, V. G., et al. 2015, *Odessa Astronomical Publications*, 28, 78. doi:10.48550/arXiv.1510.02169
- van Altena, W. F., Lee, J. T., & Hoffleit, E. D. 1995, *The General Catalogue of Trigonometric Parallaxes*, 4th Ed., (New Haven, CT: Yale Univ. Observatory)
- van Leeuwen, F. 2013, *A&A*, 550, L3
- Vogel, H., C. 1888, *Publ. des Astrophys. Obs. du Potsdam*, Bd. VII, Theil I., p. 96
- Welsh, W. F., Orosz, J. A., Aerts, C., et al. 2011, *ApJS*, 197, 4
- Wielen, R., Jahreiß, H., Dettbarn, C., et al. 2000, *A&A*, 360, 399
- Williams, J. A. 1966, *AJ*, 71, 615
- Wilson, T. D., Carter, M. W., Barnes, T. G., et al. 1989, *ApJS*, 69, 951